Carbonized Hemoglobin Functioning as a Cathode Catalyst for Polymer Electrolyte Fuel Cells

Jun Maruyama* and Ikuo Abe

Environmental Technology Department, Osaka Municipal Technical Research Institute, 1-6-50, Morinomiya, Joto-ku, Osaka 536-8553, Japan

Received August 11, 2005. Revised Manuscript Received December 8, 2005

Raw materials for producing polymer electrolyte fuel cells should be inexpensive and abundant in their resource in order to widely substitute this new energy system for conventional ones. In this study, a catalyst for the cathodic oxygen reduction was formed from hemoglobin, a large amount of which would be always available. The heat treatment in an inert atmosphere around 800 °C produced a carbonized material with highly developed nanospaces. The specific surface area reached 1005 $m^2\ g^{-1}$ at the optimized carbonization conditions. The fundamental electrochemical properties were evaluated using rotating disk electrodes, forming a catalyst layer from the carbonized material with the polymer electrolyte on the electrode surface and immersing the layer in oxygen-saturated perchloric acid. We found that the carbonized materials were active toward oxygen reduction and the activity increased with the nanospace development, essential for exposing the active sites on the pore surface. The oxygen reduction behavior reflected the pore structure and iron content. A preliminary fuel cell test using the material in the cathode confirmed the current generation. Although the performance was inferior to a Pt-based fuel cell, the result suggested that it could be improved by structure modification and surface treatment of the material.

Introduction

The substitution of conventional energy systems by fuel cells would help to improve the global environment.[1] Fuel cells generate electricity by converting chemical energy due to hydrogen combustion to electrical energy based on H_2 oxidation at the anode and O_2 reduction at the cathode, producing only water. Among the various types of fuel cells, a polymer electrolyte fuel cell (PEFC), in which perfluorosulfonate ion-exchange membranes are usually used as the electrolyte, is able to generate high power around 80 °C. This temperature range makes its start from room temperature feasible, advantageous for use as a power source of electric vehicles and cogeneration systems for domestic electricity and heating.[2−4] The PEFC has now been practically used in electric vehicles and shows promise for widespread use.

In the PEFC, H_2 oxidation (reaction 1) and O_2 reduction (reaction 2) occur as follows

$$H_2 \rightarrow 2H^+ + 2e^- \quad (1)$$

$$O_2 + 4H^+ + 4e^- \rightarrow 2H_2O \quad (2)$$

Catalysts are necessary for these reactions to occur in the electrodes, especially for the O_2 reduction due to its slow reaction rate. Nanoparticles of Pt or Pt alloys supported on electron-conductive carbon black (Pt/C) have hitherto been used as the catalyst since it has been generally recognized that only these metals are active for such reactions and stable in the highly acidic atmosphere of the polymer electrolyte. The specific surface area of Pt on the carbon black support is higher than that without the support, such as Pt black, leading to the higher PEFC performance.[5,6] The possibility of using newly developed carbon materials, such as carbon nanotubes,[7,8] carbon nanohorns,[9] and carbon nanofibers,[10−12] as catalyst supports has been recently investigated for further improvement in performance. Nevertheless, the limitation of Pt reserves and supply will prohibit widespread use of the PEFC. This has raised the demand for a catalyst that functions with far less or no Pt. There is a projection that the technology advance would decrease the Pt requirement for the PEFC to 15 g per vehicle.[13] This value corresponds to an approximately 80% decrease from the FC system in

* To whom correspondence should be addressed. Phone: +81-6-6963-8043. Fax: +81-6-6963-8049. E-mail: maruyama@omtri.city.osaka.jp.

(1) Jacobson, M. Z.; Colella, W. G.; Golden, D. M. *Science* **2005**, *308*, 1901.
(2) In *Handbook of Fuel Cells*; Vielstich, W., Lamm, A., Gasteiger, H. A., Eds.; John Wiley & Sons: Chichester, England, 2003.
(3) Costamagna, P.; Srinivasan, S. *J. Power Sources* **2001**, *102*, 242.
(4) Gottesfeld, S.; Zawodzinski, T. A. In *Advances in Electrochemical Science and Engineering*; Alkire, R. C., Gerischer, H., Kolb, D. M., Tobias, C. W., Eds.; Wiley-VCH: Weinheim, Germany 1997; Vol. 5, p 195.
(5) Wilson, M. S.; Gottesfeld, S. *J. Appl. Electrochem.* **1992**, *22*, 1.
(6) Wilson, M. S.; Gottesfeld, S. *J. Electrochem. Soc.* **1992**, *139*, L28.
(7) Li, W.; Ling, C.; Zhou, W.; Qiu, J.; Zhou, Z.; Sun, G.; Xin, Q. *J. Phys. Chem. B* **2003**, *107*, 6292.
(8) Rajesh, B.; Thampi, K. R.; Bonard, J.-M.; Xanthopoulos, N.; Mathieu, H. J.; Viswanathan, B. *J. Phys. Chem. B* **2003**, *107*, 2701.
(9) Yoshitake, T.; Shimakawa, Y.; Kuroshima, S.; Kimura, H.; Ichihashi, T.; Kubo, Y.; Kasuya, D.; Takahashi, K.; Kokai, F.; Yudasaka, M.; Iijima, S. *Physica B* **2002**, *323*, 124.
(10) Steigerwalt, E. S.; Deluga, G. A.; Lukehart, C. M. *J. Phys. Chem. B* **2002**, *106*, 760.
(11) Bessel, C. A.; Laubernds, K.; Rodriguez, N. M.; Baker, R. T. K. *J. Phys. Chem. B* **2001**, *105*, 1115.
(12) Che, G.; Lakshmi, B. B.; Fisher, E. R.; Martin, C. R. *Nature* **1998**, *393*, 346.
(13) Jaffray, C.; Hards, G. In *Handbook of Fuel Cells*; Vielstich, W., Lamm, A., Gasteiger, H. A., Eds.; John Wiley & Sons: Chichester, England, 2003; Vol. 3, Chapter 41.

10.1021/cm0517972 CCC: $33.50
Published on Web 02/09/2006

2002 and 40% consumption of the Pt reserve by full replacement of currently existing conventional vehicles. Since realization of such technology advance is unknown at present and an increase in the number of vehicles is expected, development of Pt-free catalysts is important as one approach to realize widespread use of PEFC.

It has been demonstrated in many studies that organic macrocycles such as porphyrins and phthalocyanines adsorbed on a carbon support, coordinating Fe through four central N atoms, are active for O_2 reduction but unstable in acid electrolytes and that the low stability is improved by pyrolyzing it in an inert atmosphere.[14−26] The active site of the heat-treated catalyst has been recognized as the Fe−N_x moiety that remains after heat treatment and is embedded in the carbon surface.[24−26] A few studies showed that the moiety was also formed by heat treatment of a mixture of Fe salts, carbon black, and an N-containing polymer such as polypyrrole and polyacrylonitrile.[27,28] These Pt-free catalysts are based on artificially synthesized compounds.

Recently, we produced a Pt-free catalyst from a natural organic compound, catalase, an iron enzyme consisting of four equal subunits (molecular weight: 57 000) containing the Fe(III) porphyrin.[29−33] Although catalase immobilized on glassy carbon (GC) electrodes had activity for O_2 reduction in a neutral solution,[34] this enzyme would be hydrolyzed in the highly acidic atmosphere of the polymer electrolyte.[35] However, we found that heat treatment of catalase in an inert atmosphere formed carbonized materials which were active for oxygen reduction in the highly acidic atmosphere.[36] The active sites, the Fe−N_4 moiety, were formed from Fe(III) and N atoms originating from the porphyrin contained in catalase. We also found that the active sites were finely and homogeneously dispersed in the carbon matrix due to the inherent inclusion of the Fe(III) porphyrin. The carbonized material was highly porous; the specific surface area was 790 $m^2\ g^{-1}$ under optimized conditions, which was essential for exposing the active sites on the pore surface. Nevertheless, further studies are required to improve the activity and its stability. In addition, the pore-forming mechanism remains to be clarified. Since there is no systematic study on the carbonization of proteins, it is necessary to investigate the carbonization behavior of various proteins.

In this study, we carried out the carbonization of hemoglobin, one of the iron proteins, characterized the carbonized materials, and investigated the oxygen reduction at these materials. Hemoglobin consists of two pairs of subunits, represented as $\alpha_1\alpha_2\beta_1\beta_2$, containing the Fe(III) porphyrin, and the total molecular weight is about 65 000.[37−40] Hemoglobin is easily available due to its abundance. In particular, utilization of blood from the meat industry would be promising. Almost all red blood cells in blood are discarded as waste, and the meat industry produces more than 200 million tons of meat per year around the world. The amount of hemoglobin is roughly estimated to be 2 million tons.[40] Improvement in the activity of the carbonized materials for oxygen reduction would be expected due to the higher Fe content per molecule than catalase.

We found that the carbonization of hemoglobin produced highly developed micropores inside the carbonized material in a very limited heat-treatment temperature range. Only a 25 °C change in the heat-treatment temperature caused substantial change in the specific surface area. The specific surface area was as high as 1005 $m^2\ g^{-1}$. We also found that the O_2 reduction behavior reflected the pore structure and Fe content.

Experimental Section

Materials. Hemoglobin from bovine blood was purchased from Sigma and used as received. A commercially available catalyst of 10 wt % platinum on Vulcan XC-72R carbon (ElectroChem) was used as the Pt/C material. High-purity water was obtained by circulating ion-exchanged water through an Easypure water-purification system (Barnstead, D7403). Perchloric acid (70%, Tama Chemical, analytical grade) was diluted with the high-purity water to prepare 0.1 mol dm^{-3} $HClO_4$. A solution of Nafion as a perfluorosulfonate ion-exchange resin [equivalent weight (molar mass/mol of ion-exchange site) = 1100, 5 wt % dissolved in a mixture of lower aliphatic alcohols and 15−20% water] was purchased from Aldrich. Nafion 112 was used as the electrolyte membrane for the fuel cell test. The membrane was successively immersed in 3% H_2O_2, high-purity water, 1 mol dm^{-3} H_2SO_4, and

(14) Tarasevich, M. R.; Sadkowski, A.; Yeager, E. In *Comprehensive Treatise of Electrochemistry*; Bockris, J. O'M., Conway, B. E., Yeager, E., Khan, S. U. M., White, R. E., Eds.; Plenum: New York, 1983; Vol. 7, Chapter 6.
(15) Tanaka, A. A.; Fierro, C.; Scherson, D.; Yeager, E. B. *J. Phys. Chem.* **1987**, *91*, 3799.
(16) Widelöv, A.; Larsson, R. *Electrochim. Acta* **1992**, *37*, 187.
(17) Widelöv, A. *Electrochim. Acta* **1993**, *38*, 2493.
(18) Bittins-Cattaneo, B.; Wasmus, S.; Lopez-Mishima, B.; Vielstiech, W. *J. Appl. Electrochem.* **1993**, *23*, 625.
(19) Faubert, G.; Lalande, G.; Côté, R.; Guay, D.; Dodelet, J. P.; Weng, L. T.; Bertrand, P.; Dénès, G. *Electrochim. Acta* **1996**, *41*, 1689.
(20) Lalande, G.; Faubert, G.; Côté, R.; Guay, D.; Dodelet, J. P.; Weng, L. T.; Bertrand, P. *J. Power Sources* **1996**, *61*, 227.
(21) Faubert, G.; Côté, R.; Guay, D.; Dodelet, J. P.; Dénès, G.; Bertrand, P. *Electrochim. Acta* **1998**, *43*, 341.
(22) Bouwkamp-Wijnoltz, A. L.; Visscher, W.; van Veen, J. A. R. *Electrochim. Acta* **1998**, *43*, 3141.
(23) Gojković, S. L.; Gupta, S.; Savinell, R. F. *J. Electroanal. Chem.* **1999**, *462*, 63.
(24) Lefèvre, M.; Dodelet, J. P.; Bertrand, P. *J. Phys. Chem. B* **2002**, *106*, 8705.
(25) Lefèvre, M.; Dodelet, J. P. *Electrochim. Acta* **2003**, *48*, 2749.
(26) Schulenburg, H.; Svetoslav, S.; Schünemann, V.; Radnik, J.; Dorbandt, I.; Fiechter, S.; Bogdanoff, P.; Tributsch, H. *J. Phys. Chem. B* **2003**, *107*, 9034.
(27) Gupta, S.; Tryk, D.; Bae, I.; Aldred, W.; Yeager, E. *J. Appl. Electrochem.* **1989**, *19*, 19.
(28) Côté, R.; Lalande, G.; Guay, D.; Dodelet, J. P.; Dénès, G. *J. Electrochem. Soc.* **1998**, *145*, 2411.
(29) Kiselev, N. A.; Shpitzberg, C. L.; Vainshtein, B. K. *J. Mol. Biol.* **1967**, *25*, 433.
(30) Murthy, M. R. N.; Reid, T. J., III; Sicignano, A.; Tanaka, N.; Rossmann, M. G. *J. Mol. Biol.* **1981**, *152*, 465.
(31) Reid, T. J., III; Murthy, M. R. N.; Sicignano, A.; Tanaka, N.; Musick, W. D. L.; Rossmann, M. G. *Proc. Natl. Acad. Sci. U.S.A.* **1981**, *78*, 4767.
(32) Fita, I.; Rossmann, M. G. *J. Mol. Biol.* **1985**, *185*, 21.
(33) Melik-Adamyan, W. R.; Barynin, V. V.; Vagin, A. A.; Borisov, V. V.; Vainshtein, B. K.; Fita, I.; Murthy, R. N.; Rossmann, M. G. *J. Mol. Biol.* **1986**, *188*, 63.
(34) Lai, M. E.; Bergel, A. *J. Electroanal. Chem.* **2000**, *494*, 30.
(35) Samejima, T.; Yang, J. T. *J. Biol. Chem.* **1963**, *238*, 3256.
(36) Maruyama, J.; Abe, I. *Chem. Mater.* **2005**, *17*, 4660.
(37) Ohtsuka, S.; Yamanaka, T. *Chemistry of Metal Proteins*; Koudansha: Tokyo, 1983.
(38) Fasman, G. D. *Handbook of Biochemistry and Molecular Biology*, 3rd ed.; CRC Press: Cleveland, OH, 1976; Vol. 3.
(39) Fermi, G. *J. Mol. Biol.* **1975**, *97*, 237.
(40) Harris, J. W. *The Red Cell*; Harvard University Press: Cambridge, 1965.

high-purity water at boiling temperature. The argon, hydrogen, and oxygen gases were of ultrahigh purity.

Carbonization of Hemoglobin and Characterization of the Carbonized Materials. The carbonization of hemoglobin was carried out in 100 cm^3 min^{-1} flowing Ar at 750, 775, 800, 825, and 850 °C for 2 h after raising the temperature at 5 °C min^{-1}. For convenience, the carbonized material produced at 750 °C is hereafter called CHb750, and the others are named in a similar manner. The Fe contents in the carbonized materials were measured by inductively coupled plasma atomic emission spectrophotometry (ICP-AES) using an ICPS-8100 system (Shimadzu) after combustion of the carbon matrix and dissolution of the residue by 0.5 mol dm^{-3} H_2SO_4 at boiling temperature. Treatment with an acid solution was also carried out for CHb825 to remove soluble Fe species on the surface. The treatment was performed in 0.5 mol dm^{-3} H_2SO_4 at boiling temperature for 1 h, followed by filtering, washing with high-purity water, and drying in a vacuum at room temperature. The acid-treated CHb825 is hereafter called CHb825A. The amount of Fe in the leaching solution was also determined by ICP-AES. The adsorption isotherm of N_2 onto the carbonized material was measured using an automatic N_2 adsorption apparatus (Belsorp 28, Nihon Bell) at −196 °C. The specific surface area was determined by the Brunauer−Emmet−Teller (BET) plot of the isotherm and the pore volume by the amount of adsorbed N_2 at a relative pressure of 0.931. The mean pore diameter was calculated assuming that the pore was cylindrical and using the equation

$$d = 4V_p/S$$

where d is the mean pore diameter, V_p is the pore volume, and S is the specific surface area. The differential pore-size distributions were also obtained using the isotherm. X-ray diffraction (XRD) was performed with an automated RINT 2500 X-ray diffractometer (Rigaku) using Cu Kα radiation. Data acquisition was carried out in the $\theta/2\theta$ step scanning mode at a speed of 1° min^{-1} with a step size of 0.02° (2θ). A transmission electron micrograph (TEM) was obtained using a JEM-1200EX (JEOL). X-ray photoelectron spectroscopy (XPS) was carried out using a PHI ESCA 5700 system (Physical Electronics) with Al Kα radiation (1486.6 eV) in which the finely ground carbonized material was fixed on an Al adhesive tape.

Catalyst Layer Formation. The electrochemical characteristics of the carbonized material were fundamentally investigated by fixing it on the surface of a rotating glassy carbon disk electrode (GC RDE) as a catalyst layer and immersing it in 0.1 mol dm^{-3} $HClO_4$.[41−44] An aliquot of 100 mg of the finely ground carbonized material and 10 mg of carbon black (Vulcan XC-72R, Cabot) as the electron-conductive agent were added to 1 cm^3 of the Nafion solution. The mixture was ultrasonically dispersed to produce a catalyst paste. A GC RDE (BAS), which consisted of a GC rod sealed in a Kel-F holder, was polished with a 2000 grit emery paper (Sumitomo 3M) and then ultrasonically cleaned in high-purity water for use as a support for the catalyst layer. The geometric surface area of the electrode was 0.071 cm^2 (diameter, 3 mm). A 1 mm^3 volume of the paste was pipetted onto the GC surface, and to shield it from the irregular air stream generated by a ventilator, the electrode was immediately placed under a glass cover until the layer was formed. After removal of the glass cover, the layer was further dried overnight at room temperature. A catalyst layer without the carbonized material was similarly formed from 10 mg of the carbon black and 1 cm^3 of the Nafion solution for comparison.

Electrochemical Measurements. An electrochemical analyzer (100B/W, BAS) and an RDE glass cell were used for cyclic voltammetry and measurements of the current−potential relationships. The glass cell was cleaned by soaking in a 1:1 mixture of concentrated HNO_3 and H_2SO_4, followed by a thorough rinsing with high-purity water, and finally steam cleaning.[45] The counter electrode was a Pt wire, and the reference electrode was a reversible hydrogen electrode (RHE). All potentials were referred to the RHE. Cyclic voltammograms for the catalyst layers were recorded in Ar-saturated 0.1 mol dm^{-3} $HClO_4$ at 25 °C. The potential was scanned between 0.05 and 1.3 V at a scan rate of 50 mV s^{-1}. Before recording, the potential was repeatedly scanned between 0.05 and 1.4 V to remove any residual impurities. The current−potential relationships were obtained in O_2-saturated 0.1 mol dm^{-3} $HClO_4$ at 25 °C at various rotation speeds. The scan rate of the potential was fixed at 10 mV s^{-1}. Prior to measurement, the electrode was repeatedly and alternately polarized at 0.05 and 1.3 V.[46] The potential was finally stepped to 1.2 V and then swept in the negative direction to obtain the current−potential relationship. The background current was similarly measured in an Ar atmosphere without rotation.

Fuel Cell Tests. A catalyst layer was formed on a 5 cm^2 carbon cloth or paper treated with poly(tetrafluoroethylene) (ElectroChem) as the gas-diffusion layer. A cathode was formed on the carbon cloth from CHb825 or CHb825A by spreading the paste similarly prepared as described above with a mixture of the Nafion solution and the high-purity water, followed by drying overnight at room temperature. The amounts of CHb825, the electron-conductive agent, and Nafion were 10, 1.0, and 5.0 mg cm^{-2}, respectively. An anode was formed using a catalyst paste prepared by adding Pt/C to the mixture of Nafion solution and the high-purity water and then ultrasonically dispersing it. The paste was spread on the carbon paper and dried overnight at room temperature. The amounts of Pt/C and Nafion were 1.0 (Pt, 0.1 mg cm^{-2}) and 0.5 mg cm^{-2}, respectively. A cathode of a conventional Pt-based fuel cell for performance comparison was formed on the carbon cloth in the same way. The electrodes and the electrolyte Nafion 112 membrane were pressed at 2.5 MPa and 150 °C for 10 min to form the membrane−electrode assembly, which was then incorporated into a single-cell apparatus (ElectroChem). Hydrogen and oxygen were humidified at 80 °C and passed into the apparatus at 100 cm^3 min^{-1} and atmospheric pressure. The partial pressure of hydrogen and oxygen was 54 kPa. The current−potential relationships were measured at 80 °C using a fuel cell station (NF) after a continuous 2-h operation at 0.5 V as a pretreatment. Subsequently, the current at 0.5 V was recorded during a continuous operation.

Results and Discussion

Single-Step Generation of Activated Carbon from Hemoglobin. The heat treatment of hemoglobin at 750, 775, 800, and 825 °C produced the carbonized materials in the following yields: 22.2%, 20.3%, 14.2%, and 11.5%, respectively. The yield decreased with an increase in the heat-treatment temperature. Only a trace amount was left after heat treatment at 850 °C. The Fe contents were as follows: CHb750, 0.68 wt %; CHb775, 0.77 wt %; CHb800, 1.11 wt %; CHb825, 1.37 wt %; CHb825A, 0.47 wt %.

(41) Maruyama, J.; Abe, I. *J. Electrochem. Soc.* **2004**, *151*, A447.
(42) Maruyama, J.; Abe, I. *Electrochim. Acta* **2003**, *48*, 1443.
(43) Gloaguen, F.; Andolfatto, F.; Durand, R.; Ozil, P. *J. Appl. Electrochem.* **1994**, *24*, 863.
(44) Gojković, S. Lj.; Zečević, S. K.; Savinell, R. F. *J. Electrochem. Soc.* **1998**, *145*, 3713.
(45) Chu, D.; Tryk, D.; Gervasio, D.; Yeager, E. B. *J. Electroanal. Chem.* **1989**, *272*, 277.
(46) Razaq, M.; Razaq, A.; Yeager, E.; DesMarteau, D. D.; Singh, S. *J. Electrochem. Soc.* **1989**, *136*, 385.

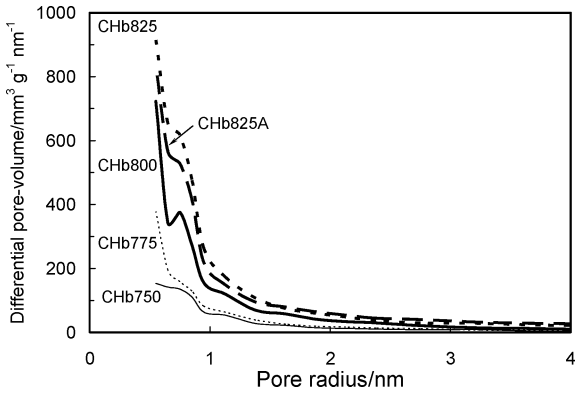

Figure 1. Pore-size distributions of CHb750 (thin line), CHb775 (thin dotted line), CHb800 (thick line), CHb825 (thick dotted line), and CHb825A (thick dashed line).

The specific surface areas and mean pore diameters determined by the N_2 adsorption isotherm were as follows: CHb750, 517 m^2 g^{-1}, 1.73 nm; CHb775, 597 m^2 g^{-1}, 1.71 nm; CHb800, 816 m^2 g^{-1}, 1.78 nm; CHb825, 1005 m^2 g^{-1}, 1.92 nm. A 25 °C difference in the heat-treatment temperature caused a significant difference in the pore structure. The surface areas of CHb800 and CHb825 were as high as that of the commercial activated carbon. In addition to these values of specific surface area and mean pore diameter, the pore-size distributions of CHb750, CHb775, CHb800, and CHb825 (Figure 1) confirmed a significant nanospace development in the carbonized material. In particular, the pore size was distributed below the pore radius of 2 nm in all carbonized materials, indicating that pore development proceeded within the very limited range of the pore radius. Generally, activated carbon is produced from coconut shells or coal through their carbonization and then an activation process using steam or CO_2. In contrast, the results in the present study indicate that activated carbon can be produced from hemoglobin by a one-step temperature-controlled heat treatment. A similar pore development also occurred for carbonization of an Fe enzyme, catalase, although the pore structure and its variation with an increase in the heat-treatment temperature were different; the pore size was more widely distributed, and the variation was slower.[36] These results suggest that the properties of the carbonized materials from proteins and the carbonization processes are dependent on the kind of raw material. Further results are being obtained in our department using various proteins to clarify the relationship between raw materials and products as well as the carbonization processes using other analytical methods such as Raman spectroscopy, which will be reported in another paper. The specific surface area and the mean pore diameter of CHb825A were 919 m^2 g^{-1} and 2.08 nm, respectively. The slight change in these values compared to those of CHb825 might be associated with removal of the soluble species in acid solution, which was identified below.

Iron-Containing Species in Carbonized Material. Figure 2 shows the X-ray diffraction (XRD) spectra of the carbonized materials. The large broad peaks at $2\theta = 25°$ and small broad peaks 44° were observed for all the carbonized materials. Those peaks were attributed to amorphous carbon,[47] usually observed for activated carbon. No peaks were observed except for those broad peaks in the XRD spectra of CHb750 and CHb775, whereas sharp peaks appeared in the XRD spectra of CHb800 and CHb825. These peaks were attributed to the Fe_2O_3 particles, which were formed through decomposition of the Fe(III) porphyrin and combination of Fe and oxygen from the polypeptide chains in the hemoglobin during the carbonization process. The peak growth and sharpening, which were observed in the XRD spectrum of CHb825 compared with CHb800, indicates that more Fe_2O_3 particles were present in CHb825 with their larger size than in CHb800. The Fe_2O_3 peaks disappeared in the XRD spectrum of CHb825A due to removal of Fe_2O_3 by acid treatment.

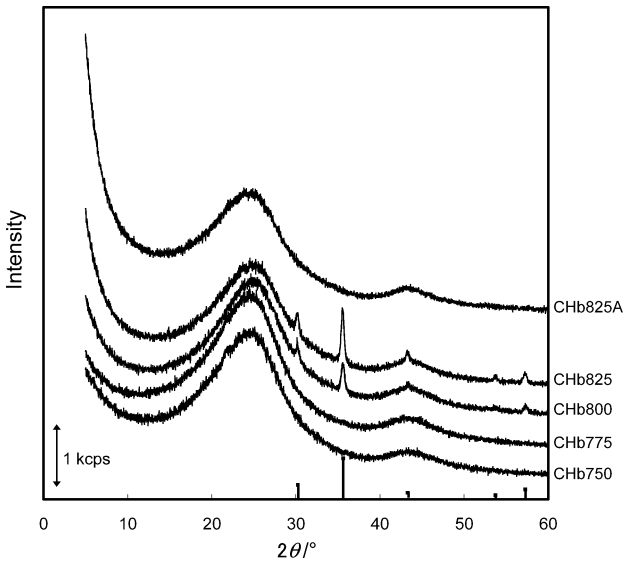

Figure 2. X-ray diffraction spectrum of CHb750, CHb775, CHb800, CHb825, and CHb825A. Each spectrum was arbitrarily shifted for easier comparison. The positions and relative intensities of the main diffraction peaks of γ-$Fe2O_3$ (JCPDS No. 39-1346) are also shown.

Formation and removal of the Fe_2O_3 particles were also confirmed by the transmission electron micrographs of the carbonized materials shown in Figure 3. The amorphous carbon appeared as the gray areas and the Fe_2O_3 particles appeared as the black particles. The black particles were scarcely observed in the micrographs of CHb750 and CHb775 but clearly observed in those of CHb800 and CHb825. The number and size of the Fe_2O_3 particles increased in CHb825 compared with CHb800. These results indicate the generation and growth of the Fe_2O_3 particles with an increase in the heat-treatment temperature, even with the 25 °C increase.

The surfaces of the carbonized materials were characterized by X-ray photoelectron spectroscopy. Figure 4a shows the X-ray photoelectron spectrum of N 1s. The peaks at 398.2 and 400.7 eV were attributed to the N atom included in the pyridine- and pyrrole-like surface groups, respectively.[48] Figure 4b shows the X-ray photoelectron spectra of Fe 2p. Peaks at 711.3 eV for Fe $2p_{3/2}$ and 725.0 eV for Fe $2p_{1/2}$ were observed. The peak at 711.3 eV was attributed to

(47) Bron, M.; Radnik, J.; Fieber-Erdmann, M.; Bogdanoff, P.; Fiechter, S. *J. Electroanal. Chem.* **2002**, *535*, 113.
(48) Casanovas, J.; Ricart, J. M.; Rubio, J.; Illas, F.; Jiménez-Mateos, J. M. *J. Am. Chem. Soc.* **1996**, *118*, 8071.

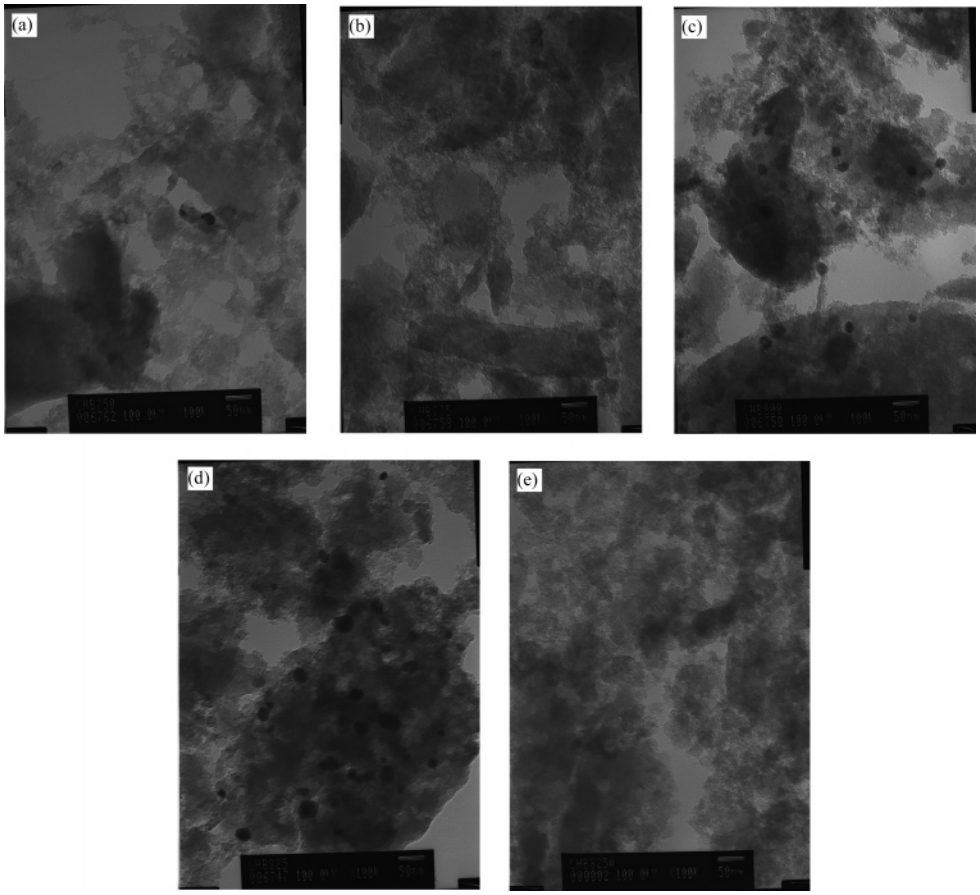

Figure 3. Transmission electron micrographs of (a) CHb750, (b) CHb775, (c) CHb800, (d) CHb825, and (e) CHb825A. Acceleration voltage was 100.0 kV. The scale bars in the micrograph correspond to 50 nm.

Fe(III) according to the value reported in the literature: 710.8−711.8 eV.[49,50] The spectra for CHb800 and CHb825 were apparently in agreement with the presence of Fe_2O_3 species. However, the peaks were also attributable to species other than Fe_2O_3 since the peak position was the same in the spectra for CHb750 and CHb775, in which the Fe_2O_3 particles were almost absent, as shown in the XRD spectra and the TEM images, and Fe might be finely dispersed in the carbon matrix. The X-ray photoelectron spectrum of Fe 2p in CHb825A (Figure 4c), which indicated the same valence state, supported the hypothesis since acid treatment could reduce the influence of the Fe_2O_3 particles, although they might be still present after the treatment.[26]

The finely dispersed Fe-containing species were probably the $Fe-N_4$ moiety embedded in the carbon surface. In our preceding study, an iron enzyme, catalase, was carbonized.[36] The presence of the moiety in the carbonized catalase was expected by retention of porphyrin-like structures in carbonaceous compounds after pyrolysis of their precursor containing metal porphyrins[16,51,52] and also implied by the Mössbauer spectrum of the carbonized catalase. The presence of the moiety was expected similarly in the carbonized material in this study.

Cyclic Voltammetry. Figure 5 shows the cyclic voltammograms for the catalyst layers in Ar-saturated 0.1 mol dm^{-3} $HClO_4$, which provides information on the electrochemical surface properties of the carbonized materials in contact with the polymer electrolyte. The sign of the current due to the oxidation reactions was taken as positive, and that due to the reduction reactions was taken as negative. The current in both the positive and negative scans increased with an increase in the heat-treatment temperature. Charging of the electrochemical double layer might mostly cause the current due to the large surface area of the carbonized material. In addition, two kinds of peaks were observed in the voltammograms for the CHb800 and CHb825 layers. Very broad peaks were attributable to the redox reaction of quinone-like functional groups (Q) on the surfaces, which is usually observed for carbon electrodes[53]

$$Q + 2H^+ + 2e^- \leftrightarrow QH_2 \qquad (3)$$

The very small peaks attributed to the $Fe^{2+/3+}$ redox reaction were overlapped on the broad peaks and situated at 0.75 V in the positive scan and 0.65 V as a shoulder in the negative scan. These Fe species might be derived from the $Fe-N_4$ moiety or the Fe_2O_3 particles through the dissolution and reduction during the potential cycles. Those peaks were not observed in the voltammogram for the CHb825A layer, indicating that acid treatment removed the soluble Fe species.

(49) Johansson, L. Y.; Larsson, R. *Chem. Phys. Lett.* **1974**, *24*, 508.
(50) Choudhury, T.; Saied, S. O.; Sullivan, J. L.; Abbot, A. M. *J. Phys. D: Appl. Phys.* **1989**, *22*, 1185.
(51) Jones, J. M.; Zhu, Q.; Thomas, K. M. *Carbon* **1999**, *37*, 1123.
(52) Herod, A. J.; Gibb, T. C.; Herod, A. A.; Xu, B.; Zhang, S.; Kandiyoti, R. *Fuel* **1996**, 75, 437.
(53) Maruyama, J.; Abe, I. *Electrochim. Acta* **2001**, *46*, 3381.

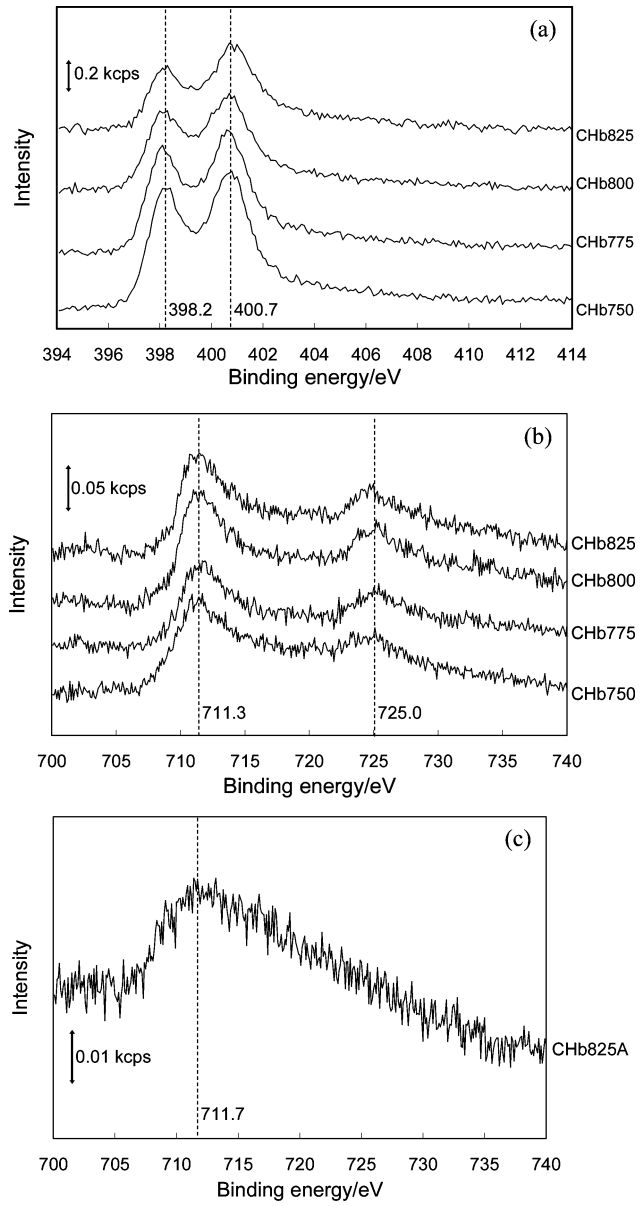

Figure 4. X-ray photoelectron spectra of N 1s (a) and Fe 2p (b) in CHb750, CHb775, CHb800, and CHb825 and Fe 2p in CHb825A (c). Each spectrum was arbitrarily shifted in the *y*-axis direction for easier comparison.

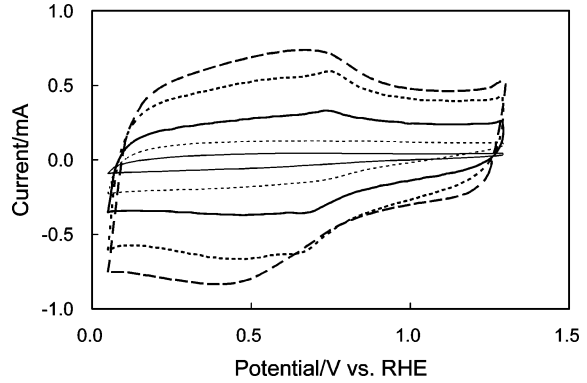

Figure 5. Cyclic voltammograms for catalyst layers formed from CHb750 (thin line), CHb775 (thin dotted line), CHb800 (thick line), CHb825 (thick dotted line), and the acid-treated CHb825 (thick dashed line) in Ar-saturated 0.1 mol dm^{-3} $HClO_4$ at 25 °C. Scan rate: 50 mV s^{-1}.

The increase in the current in this voltammogram might be due to removal of the Fe_2O_3 particles, which allowed deeper penetration of Nafion molecules into the pore of the carbonized material. The $Fe^{2+/3+}$ redox peaks were also absent in the voltammograms for the CHb750 and CHb775 layers. The low surface areas of CHb750 and CHb775 limited the number of quinone-like surface functional groups, and the insufficient development of pores limited exposure of the $Fe-N_4$ moiety to the pore surface, which resulted in almost eliminating the peaks.

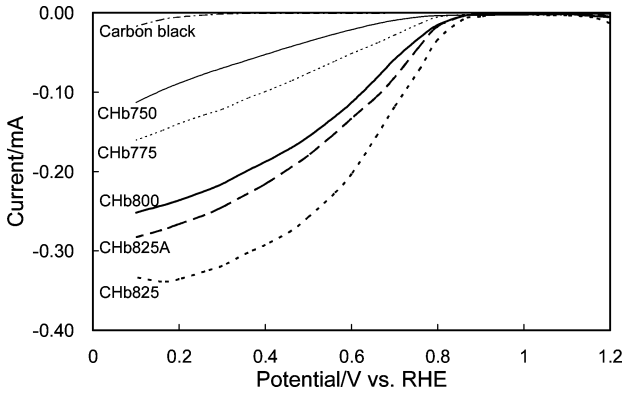

Figure 6. Relationships between electrode potential and oxygen reduction current of negative scans at catalyst layers formed from CHb750 (thin line), CHb775 (thin dotted line), CHb800 (thick line), CHb825 (thick dotted line), CHb825A (thick dashed line), and carbon black (thin chain line) in O_2-saturated 0.1 mol dm^{-3} $HClO_4$ at 25 °C. Scan rate: 10 mV s^{-1}. Electrode rotation speed: 2000 rpm.

Oxygen Reduction. Oxygen reduction currents at the catalyst layers were measured in O_2-sarturated 0.1 mol dm^{-3} $HClO_4$ with the electrodes being rotated at various rotation speeds. Figure 6 shows the relationships between the electrode potential and currents at the catalyst layers formed from CHb750, CHb775, CHb800, CHb825, CHb825A, and only an electron-conductive agent, measured by rotating the electrodes at 2000 rpm. The current shown in Figure 6 was obtained by subtracting the background current from the measured current. The O_2 reduction currents at the catalyst layers formed from the carbonized material increased with an increase in the heat-treatment temperature. The current was smaller at the CHb825A layer than that at the CHb825 layer. These currents shown in Figure 6 arose from the O_2 reduction inside the catalyst layer but included the influence of the mass transfer in the 0.1 mol dm^{-3} $HClO_4$ solution in which the catalyst layer was immersed. The activities of the catalyst layers for O_2 reduction were evaluated using the reduction current free of the influence of the mass transfer in the solution, I_K, determined by[42]

$$-\frac{1}{I} = -\frac{1}{I_K} + \frac{1}{0.620nFAD^{2/3}c\nu^{-1/6}\omega^{1/2}}$$

where I is the reduction current after subtracting the background current, n is the number of electrons involved in the O_2 reduction per molecule, F is the Faraday constant, A is the geometric area of the GC electrode, D is the diffusion coefficient of O_2 in solution, c is the concentration of O_2 in solution, ν is the kinematic viscosity of the solution, and ω is the angular frequency of rotation. Figure 7 shows $-1/I$ vs $\omega^{-1/2}$ plots for the O_2 reduction at 0.1 V and n that were calculated using the slope of the plot and the following

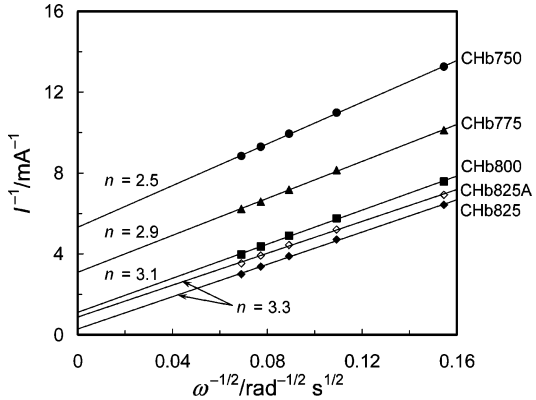

Figure 7. $-1/I$ vs $\omega^{-1/2}$ plots for oxygen reduction and number of electrons involved in the reaction per molecule at 0.1 V for catalyst layers formed from CHb750 (●), CHb775 (▲), CHb800 (■), CHb825 (◆), and CHb825A (◇).

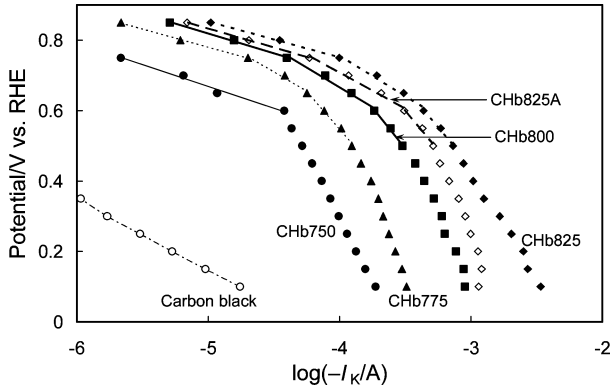

Figure 8. Relationships between electrode potential and log($-I_K/A$) for catalyst layers formed from CHb750 (●), CHb775 (▲), CHb800 (■), CHb825 (◆), and CHb825A (◇). Relationship for catalyst layer formed only from carbon black (○) is also shown for comparison.

values:[54−56] F, 96485 C mol^{-1}; A, 0.0707 cm^2; D, 1.9×10^{-5} cm^2 s^{-1}; c, 1.18×10^{-6} mol cm^{-3}; ν, 9.87×10^{-3} cm^2 s^{-1}. A two-electron reduction generates the intermediate H_2O_2 (reaction 4). An increase in n occurs with its further reduction (reaction 5), the decomposition of H_2O_2 (reaction 6), or an increase in the proportion of the four-electron reduction to H_2O (reaction 2)[57]

$$O_2 + 2H^+ + 2e^- \rightarrow H_2O_2 \quad (4)$$

$$H_2O_2 + 2H^+ + 2e^- \rightarrow 2H_2O \quad (5)$$

$$2H_2O_2 \rightarrow 2H_2O + O_2 \quad (6)$$

At the CHb750 layer n was 2.5, indicating that the two-electron reduction predominated and the oxygen reduction occurred mainly on the carbon surface of the carbonized material.[14] The number of electrons increased with an increase in the heat-treatment temperature: 2.9 at the CC775 layer, 3.1 at the CHb800 layer, and 3.3 at the CHb825 layer. The development of micropores exposed the Fe−N_4 moiety in the carbonized material to the pore surface, which led to the increase in the number of active sites. This increase then raised the possibility that H_2O_2 molecules generated inside the catalyst layer were further reduced (reaction 5) or decomposed (reaction 6) during their transfer to the outside of the layer, which resulted in the n increase. The change in n was not observed after acid treatment of CHb825. Reduction of the particle size of the carbonized material by thorough grinding would further increase n due to an increase in the possibility of contact between the H_2O_2 molecules and the active sites. The studies regarding the n increase are currently underway.

The relationships between electrode potential and log($-I_K/A$) (Tafel plots) are shown in Figure 8. The activity for O_2 reduction at the catalyst layers formed from the carbonized material increased with an increase in the heat-treatment temperature. The increase in the number of active sites caused by the development of micropores could essentially produce the increase in $-I_K$. Since the activity of Fe_2O_3 for oxygen reduction was very low,[58] the contribution of the particles in the carbonized materials to the current could be neglected. Another possible reason for the $-I_K$ increase is the intrinsic activity increase in the Fe−N_4 moiety. It has been reported that the activity of the catalyst prepared by heat treatment of the iron porphyrins adsorbed on carbon materials depends on the heat-treatment temperature and reaches a maximum when the temperature is around 800 °C.[19,20,23−25] However, an activity change as large as that shown in this study with a 25 °C change in the heat-treatment temperature near the maximum activity has not been reported before. Therefore, the main reason for the activity increase was attributable to the increase in the active sites. The activity was decreased by acid treatment of CHb825, probably due to the loss of the active sites, although the activity was still higher than that of the CHb800 layer.

A further increase in $-I_K$ in the low potential region by adsorption of CF_3SO_3H in the pores of CHb825 was expected according to previous studies, which reported that the presence of CF_3SO_3H improved the mass transfer in the pores of activated carbon[41] and the carbonized catalase.[36] However, no improvement was observed for CHb825. It was recently found that the effect of CF_3SO_3H was dependent on the kinds of activated carbon.[59] CHb825 was presumably unsuitable for CF_3SO_3H treatment, although a detailed reason is not clear at present.

In contrast, $-I_K$ at the CHb825 layer in the high potential region was about three times higher than that at the layer formed from the carbonized catalase with optimum activity. Although not all the irons in hemoglobin were transformed to the active sites, the higher Fe content in hemoglobin than in catalase might contribute to the improved activity. In addition, the higher specific surface area of the carbonized hemoglobin than that obtained for carbonized catalase would be another reason for the improvement. We recently found that oxygen reduction at a catalyst layer formed from activated carbon loaded with platinum was enhanced by the increased specific surface area of the activated carbon.[60]

(54) Maruyama, J.; Abe, I. *J. Electroanal. Chem.* **2003**, *545*, 109.
(55) Zečević, S. K.; Wainright, J. S.; Litt, M. H.; Gojković, S. Lj.; Savinell, R. F. *J. Electrochem. Soc.* **1997**, *144*, 2973.
(56) Mello, R. M. Q.; Ticianelli, E. A. *Electrochim. Acta* **1997**, *42*, 1031.
(57) Maruyama, J.; Inaba, M.; Morita, T.; Ogumi, Z. *J. Electroanal. Chem.* **2001**, *504*, 208.
(58) Balko, B. A.; Clarkson, K. M. *J. Electrochem. Soc.* **2001**, *148*, E85.
(59) Maruyama, J.; Abe, I. *J. Power Sources* **2005**, *148*, 1.
(60) Maruyama, J.; Abe, I. *Carbon* **2004**, *42*, 3115.

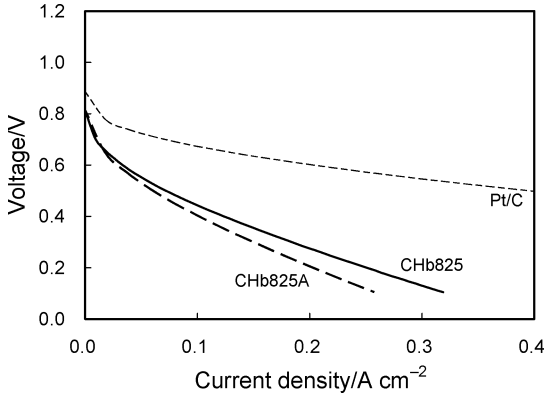

Figure 9. Relationships between cell voltage and currents generated by fuel cells formed from CHb825 (thick line), CHb825A (thick dashed line), and Pt/C (thin dashed line). Cell temperature: 80 °C. Hydrogen and oxygen were humidified at 80 °C and passed into the cell apparatus at 100 cm^3 min^{-1} and atmospheric pressure. The partial pressure of hydrogen and oxygen was 54 kPa.

Since the carbonized catalase and hemoglobin possessed specific surface areas as high as activated carbon, it might be valid to presume that a similar behavior also occurred at the catalyst layer formed from the carbonized hemoglobin.

The Tafel plots showed several linear regions. The slopes of the lines (Tafel slope) for the CHb825 layer were −0.10, −0.23 V, and −0.44 V decade^{-1} from the high to low potential region. The value of −0.10 V decade^{-1} was close to the value of −0.12 V decade^{-1}, which indicated that the rate-determining step of O_2 reduction at the carbonized materials was the step of the first electron transfer to an O_2 molecule adsorbed on the surface following the Langmuir isotherm.[61] Further detailed mechanisms will be discussed after accumulation of the data by the investigation of oxygen reduction at various Fe-based Pt-free catalysts formed from various raw materials.

The increase in the Tafel slopes observed with a decrease in the electrode potential could be explained by the flooded-agglomerate model proposed by Perry et al.,[62] which predicts that a double Tafel slope will be observed in a potential region where O_2 reduction is controlled by kinetics and diffusion of dissolved O_2 and a quadruple Tafel slope in a region where O_2 reduction is controlled by kinetics, the diffusion of dissolved oxygen, and ionic transfer. The two higher Tafel slopes, −0.23 and −0.44 V decade^{-1}, therefore correspond to the double and quadruple Tafel slopes, respectively, although the model does not fully agree with the behavior in this study, which showed first-order kinetics in oxygen concentration across all potential regions.[44] The Tafel plot for the CHb750 layer showed only one Tafel slope (−0.12 V decade^{-1}) that followed the theory. The $-I_K$ increase with a decrease in the electrode potential was slow below that region, probably due to the insufficiently developed pores that might hinder the mass transfer.

Fuel Cell Test. Preliminary fuel cell tests were carried out by forming cathodes from CHb825, CHb825A, and Pt/C. Figure 9 shows the relationships between the cell potential and the currents generated by the fuel cells. The amount of Pt in the cathode formed from Pt/C was nearly equal to that of Fe in the cathode formed from CHb825. These results confirmed that the single cell formed from the carbonized material generated current, although the performance was inferior to that of the conventional Pt/C fuel cell. The performance declined during continuous operation at 0.5 V (Figure 10); the current significantly decreased during the first 24 h, 52% of the initial current, and gradually decreased to 41% at 48 h. The current decrease is probably attributed to destruction of the active sites.[25,26] However, the performance was improved compared to that of the fuel cell whose cathode was formed from carbonized catalase, except in the very low potential region, below 0.2 V.[36] In particular, the current in the high potential region was three times higher, in agreement with the results obtained using rotating disk electrodes. The current retention ratio after the 48-h operation was also improved from 36% to 41%.

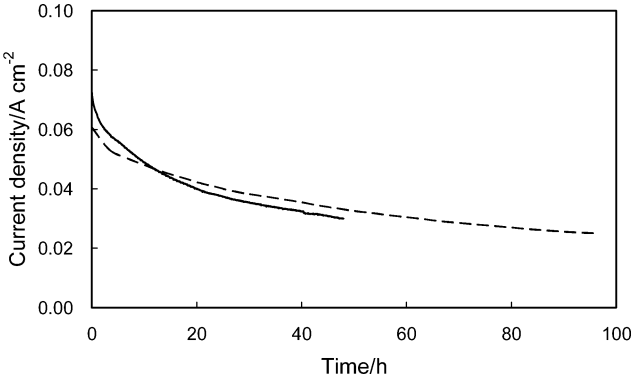

Figure 10. Current change in fuel cells formed from CHb825 (solid line) and CHb825A (dashed line) during continuous operation at 0.5 V. Cell temperature: 80 °C. Hydrogen and oxygen were humidified at 80 °C and passed into the cell apparatus at 100 cm^3 min^{-1} and atmospheric pressure. The partial pressure of hydrogen and oxygen was 54 kPa.

The current decrease was further slower at the fuel cell formed from CHb825A, although the initial current was lower than that at the fuel cell formed from CHb825, which reflected the activity loss, and the reason for the improvement is not clear at present. The 48% and 59% decrease observed at 24 and 48 h for the fuel cell formed from CHb825 were observed at 55 and 98 h for the fuel cell formed from CHb825A, respectively, indicating the acid treatment is one approach to improve durability of the carbonized material as a cathode catalyst. On the basis of the results on the carbonized hemoglobin and catalase, improvement in the activity and durability would also be expected by modifying the carbonizing condition, for instance, the atmosphere and heating rate, which leads to modification of the structure of the carbonized material. Further studies are being done to investigate these variables. It should also be noted that the parameters for the cathode catalyst layer formation, such as particle size of the carbonized material and composition, i.e., the amount of the carbonized material, the electron-conductive agent, and polymer electrolyte, were not optimized. Their optimization would further improve the performance.

Conclusions

The carbonization of hemoglobin was possible in flowing Ar, and the carbonized material possessed highly developed

(61) Sepa, D. B.; Vojnovic M. V.; Damjanovic, A. *Electrochim. Acta* **1980**, *25*, 1491.
(62) Perry, M. L.; Newman, J.; Cairns, E. *J. Electrochem. Soc.* **1998**, *145*, 5.

nanospaces inside the material. The specific surface area increased with an increase in the heat-treatment temperature and reached 1005 $m^2\ g^{-1}$, as high as that of conventional activated carbon, for the material carbonized under optimized conditions. Only a 25 °C change in the heat-treatment temperature caused a substantial change in the specific surface area. The nanospaces mainly consisted of pores whose radius was below 2 nm due to specificity of the pore-development process.

The electrochemically active surface area of the catalyst layer formed from the carbonized material increased with an increase in the heat-treatment temperature of hemoglobin carbonization, which is in agreement with an increase in the specific surface area of the carbonized material. The catalyst layer exhibited an activity for oxygen reduction. The carbonization of hemoglobin simultaneously produced the active sites and a carbon matrix as the support of the active sites. The activity also increased with an increase in the heat-treatment temperature. Pore development exposed the active sites to the pore surface, the main reason for the increase. The oxygen reduction behavior reflected the high specific surface area and the Fe content. A preliminary fuel cell test confirmed that the carbonized material could be used in the cathode to generate electricity, although the performance was inferior to that of a conventional Pt/C fuel cell. However, the performance was improved compared to the fuel cell formed from carbonized catalase due to the higher specific surface area and Fe content, and a better result was also obtained for the continuous operation of the fuel cell, suggesting that modification of the structure of the carbonized material would improve its performance and durability. Surface treatment of the carbonized material by an acid solution also improved the durability.

Acknowledgment. We thank Mr. H. Kawano for the ICP-AES measurements, Dr. M. Izaki, Dr. M. Yamamoto, and Mr. T. Sinagawa for their help with the XRD measurements, Dr. M. Fukuzumi for his help with the TEM measurements, and Dr. M. Chigane for his help with the XPS measurements. We also thank Dr. H. Yamanaka for the discussions on proteins.

CM0517972